TN
3153

NAVAL ELECTRONICS LABORATORY CENTER, SAN DIEGO, CALIFORNIA 92152

TN 3153

AN ASSESSMENT OF RADIO PROPAGATION AFFECTED BY HORIZONTAL CHANGES IN REFRACTIVITY

3 May 1976

LCDR D. F. Glevy
Propagation Division
(Code 2200)

NELC M113

NELC TECHNICAL NOTE

THIS IS A WORKING PAPER GIVING TENTATIVE INFORMATION ABOUT SOME WORK IN PROGRESS AT NELC. IF CITED IN THE LITERATURE THE INFORMATION IS TO BE IDENTIFIED AS TENTATIVE AND UNPUBLISHED.

CONTENTS

		Page
1.	Introduction	1
2.	Approach	4
3.	Summary of Results	6
4.	San Diego Off-Shore Area Data	8
5.	San Nicolas to San Clemente Data	11
6.	San Diego High Altitude Data	17
7.	Guadalupe Data	22
8.	Canterbury Data	26
9.	Conclusions	33
10.	Acknowledgements	34
11.	References	35
12.	Bibliography	36

INTRODUCTION

Microwave radio propagation in the Navy's marine operating environment frequently exhibits unexpected behavior. The propagation anomalies are usually caused by non-standard vertical refractivity profiles. Many Navy microwave radio systems require accurate predictions of field strength within a few hundred kilometers of the transmitter, particularly along low elevation angles, because of the potentially serious effect of propagation anomalies on tactical warfare. A major advancement in this problem in recent years is the development of computer codes which can produce accurate field strength values at all elevation angles out to any desired range. However, these predictions require that the radio refractive index varies significantly only in the vertical or that the propagation medium be horizontally homogeneous since current computer codes can only incorporate one vertical refractive index profile at all horizontal ranges.

One of the most promising methods of applying the radio field strength computer codes to provide the Navy an onboard capability to assess the effect of atmospheric refractive anomalies on sensor performance is through the Integrated Refractive Effects Prediction System (IREPS) now being developed at NELC. The success of this system critically depends on the availability of a timely refractive index profile along the radio path and on the validity of the assumption that predictions based on the single profile will be realistic.

The atmosphere is generally assumed to be horizontally homogeneous in the mesoscale range (horizontal dimensions less than 300 km) for most meteorological purposes compared to the much greater changes in the vertical. This assumption can apply to the radio refractive index since examination of most climatic data indicates one must travel 500 km on the earth's surface to obtain the same refractive index change one observes travelling 1 km in the vertical.

The obvious great potential of IREPS for the Navy requires that the validity of the assumption of horizontal homogeneity as it applies to microwave radio propagation in the mesoscale range be examined. This paper examines several types of radio measurements from previously conducted experiments to assess the validity of assuming horizontal homogeneity in the marine environment Horizontal variations of meteorological elements are not the major concern of this paper. Primarily the radio field strength data are examined to determine the validity of the following specific hypothesis: "PREDICTIONS OF RADIO-FIELD STRENGTH ENHANCEMENT BEYOND THE HORIZON BASED ON A SINGLE REFRACTIVITY PROFILE AND THE ASSUMPTION OF HORIZONTAL HOMOGENEITY ARE CORRECT A MAJORITY OF THE TIME." A majority is defined as greater than 50 percent of the time. Toward this end, the following data from previously conducted experiments were analyzed:

1. Measurements at 3 GHz taken in the San Diego off-shore area utilizing a one-way propagation link between an airborne receiver and a ground-based transmitter.
2. A dual propagation link at 2.7 and 9.6 GHz between San Nicolas and San Clemente Islands operated during three test periods.
3. Measurements of radiation at 218, 418 and 1089 MHz from a high-flying jet aircraft making constant altitude flights between 8.7 and 11.9 km over the ocean in the San Diego off-shore area.
4. Data compiled by a radio meteorological team working from September 1946 through November 1947 on a line out-to-sea perpendicular to the Canterbury plain on the South Island of New Zealand.
5. Over-water transmission studies at various frequencies utilizing a transmitter-equipped PBY-5A aircraft and receivers placed at elevations

of 30 and 152 meters. Space variations of the received fields were recorded between June 1947 and June 1949.

The evaporation duct which is formed just above the surface of the ocean by the vertical distribution of moisture from evaporation of sea water and which significantly affects microwave propagation in the higher frequency ranges will not be treated in this study since the horizontal homogeneity of this duct has already been reasonably well established. (References 1 through 5)

The term "trapping layer" as used in this study is defined to be a vertical region wherein the value of refractivity (N) decreases at a rate greater than 157 units per kilometer causing the radio waves to curve downward more than the curvature of the earth and thus become trapped below this layer. The waveguide-like region of trapped energy in and below the trapping layer is called a duct. The confinement of energy in such a duct is the means by which the intensity of a radio signal can be enhanced at ranges exceeding the radio horizon.

Modified refractivity M is calculated using the relationship

$$M = (n-1)X10^6 + \frac{h}{a} 10^6,$$

where n is refractivity, h is height, and a is the earth radius.

It should be noted that there are, of course, some locations where pronounced mesoscale flows will produce quite inhomogeneous refractivity distributions, however, these locations are relatively rare in open ocean areas.

APPROACH

The ideal approach to assess the assumption of horizontal homogeneity would be to compare the results of proven radio field strength models which do not include horizontal variation with those that do for a wide variety of refractive conditions. If the radio fields calculated by the model which includes the variations of refractivity along the path do not seriously differ from the fields calculated assuming horizontal homogeneity in a majority of the cases, it could be concluded that the assumption of horizontal homogeneity is reasonable and that predictions based on it will be realistic. Unfortunately models which allow for the horizontal variation of refractivity do not exist, consequently a less rigorous method must be used to address the question.

The method used in this study is a very simple approach which first examines a single modified refractivity (M) profile associated with the radio-field strength or path-loss measurements. Based on the existence or non-existence of a ducting condition, a prediction of signal enhancement or no signal enhancement beyond the horizon was made. The requirements for the prediction of enhancement of the radio signal beyond the horizon are A) a ducting condition exists as determined by the M profile and B) the transmitter or receiver is in or within 30 m of the duct. If neither requirement is met the prediction will be "no enhancement". The radio field strength/path loss measurements were then examined to determine the accuracy of the predictions. The criterion used to determine the presence of signal enhancement was that the average signal strength out to the maximum range measured or twice the radio horizon distance, whichever is closer, must be no less than 20 db below the free space level calculated at 2 times the radio horizon distance. The assumption of horizontal homogeneity of refractive index is considered to be reasonable and the specific hypothesis stated earlier is valid if the predictions match the observations in a majority of cases.

The modified refractivity (M) profile was used in all cases because the size and location of ducts can be readily determined by constructing a vertical line tangent to a minimum point in the M curve which is the top of the duct down to the surface or in the case of an elevated duct from the point of tangency down to the point of intersection with the M curve itself.

SUMMARY OF RESULTS

A summary of the results of the rigorous application of the method chosen to test the hypothesis concerning horizontal homogeneity of the radio refractive index is given in table 1. The summary shows that the prediction of enhancement or nonenhancement of radio signal strength based on a single refractive index profile is reasonable in a majority of the cases. The method consistently produces accurate predictions in the majority of cases, despite the stringent criteria used. Even the worst success rate of 70% in the San Nicolas to San Clemente X-band data is still well above the 50% majority required.

The overall data group independent success rate calculated by using the total number of correct predictions divided by the total number of predictions made is 85.6%, while the average success rate for the five groups is 84%.

SUMMARY OF RESULTS

Data Sample	Number of Predictions	Number Correct	Percent
San Diego 3 GHz	43	39	91
San Nicolas to San Clemente			
S band	53	45	85
X band	53	37	70
San Diego Hi Alt.			
418 MHz	7	5	71
1089 MHz	8	6	75
Guadalupe Data	16	16	100
Canterbury Data			
S band	75	65	87
X band	72	67	93
Totals	327	280	85.6

Table 1. The number of cases of signal enhancement/nonenhancement predicted compared to the number observed for each data sample. The percent is the percent of correct predictions. The method of prediction is given in the text.

SAN DIEGO OFF SHORE AREA

The data collected at the San Diego off-shore area was taken utilizing a one-way propagation link between an airborne receiver and a ground based transmitter. The aircraft flew entirely over the ocean on a true line of bearing of 261° either toward or away from the transmitter. The received signal intensity was recorded on a strip chart as a function of time. The field strength was measured at several altitudes ranging from 15 to 4575 m MSL. Transmitter height was a constant 20.7 m MSL.

A frequency stabilized 3087.7 MHz transmitter and receiver were used in the experiment. Meteorological data consisted of the temperature and humidity profile taken by standard 403 MHz radiosondes at the transmitter site at times close to the flight time. Data was collected over a four month period during which trapping is likely to occur off Southern California.

Figure 1 shows typical refractivity N, and modified refractivity M as a function of height and the associated duct location calculated from a radiosonde. The profiles shown correspond closely to the time of the typical data sample shown in figure 2. Figure 2 is a plot of the measured path loss, a ratio expressed in decibels of transmitted to received power using idealized isotropic antennas, as a function of range. Shown also by the dashed line is the loss expected in free space. The letter H shown at about the 238 km point denotes the calculated radar horizon for this case.

Table 2 shows the results of testing the hypothesis of horizontal homogeneity for this data. All of the San Diego offshore area data is found in reference 6.

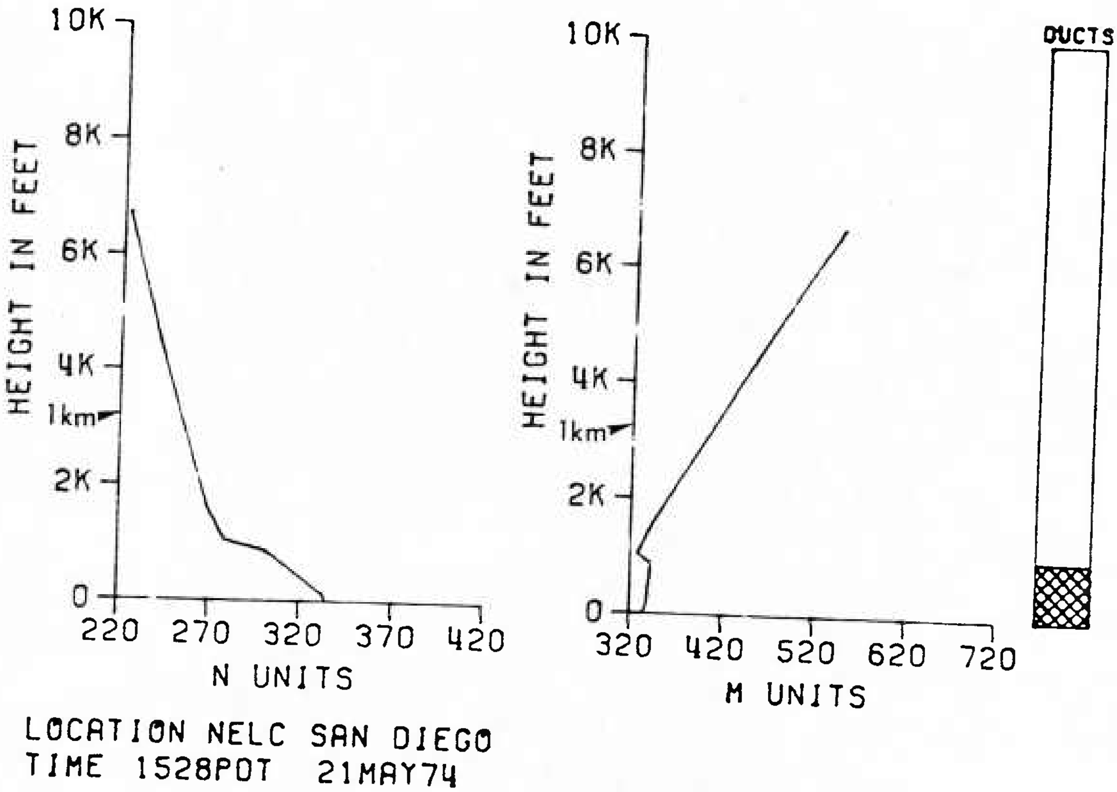

Figure 1. Sample of Refractivity (N) and Modified Refractivity (M) profiles from San Diego 3 GHz Data (Ref. 6)

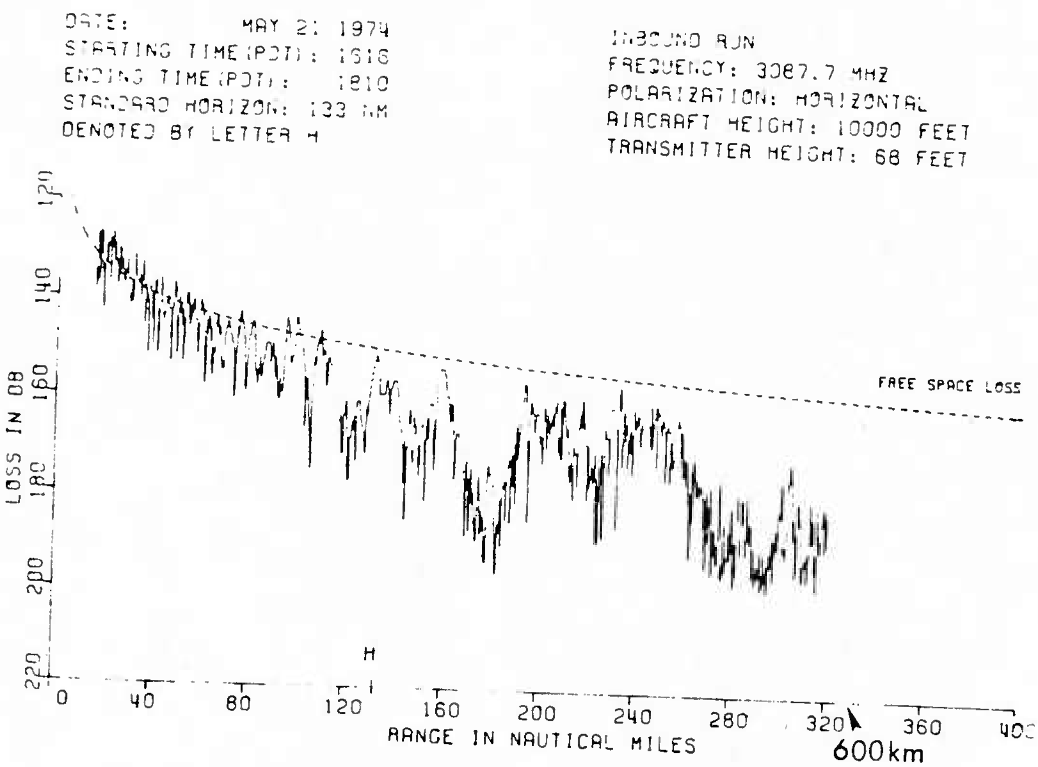

Figure 2. Sample plot of path loss as a function of range from San Diego 3 GHz data (Ref. 6)

Flight Data			Refractivity	Enhancement	
Date	Time (PDT)	Alt. (m)	Obs. Time (PDT)	Prediction	Observation
16 May 74	1056-1250	305	1233	No	No
	1255-1329	1520	1233	No	No
	1338-1405	1520	1415	No	No
	1428-1504	1520	1415	No	No
	1506-1524	1520	1415	No	--*
	1531-1554	1520	1415	No	--*
21 May	1335-1549	305	1528	Yes	Yes
	1616-1810	3050	1528	Yes	Yes
28 May	1153-1440	915	1209	No	No
	1446-1630	915	1547	No	No
11 Jun	1234-1420	1520	1143	No	No
	1430-1621	3050	1506	No	Yes
13 Jun	1249-1429	3050	1304	No	Yes
	1429-1619	1520	1517	Yes	No
	1702-1730	152	1517	Yes	Yes
2 Jul	1235-1425	1520	1310	No	No
	1443-1620	3050	1508	No	No
	1648-1720	152	1508	No	No
	1726-1801	152	1508	No	No
9 Jul	1448-1620	3050	1322	No	No
	1631-1746	3050	1546	No	No
8 Aug	1436-1559	4573	1526	No	No
	1608-1720	4573	1526	No	No
	1739-1759	30.5	1526	No	No
	1803-1823	4573	1526	No	No
13 Aug	0924-1109	4573	1220	No	No
	1116-1234	4573	1220	No	No
	1302-1327	30.5	1220	No	No
	1332-1358	30.5	1220	No	No
	1535-1723	1520	1559	No	Yes
	1736-1910	1067	1559	No	No
14 Aug	0827-0951	945	0917	Yes	Yes
	0953-1113	915	0917	Yes	Yes
	1121-1209	305	1117	Yes	Yes
	1214-1256	305	1117	Yes	Yes
	1414-1436	15.2	1315	No	No
	1439-1458	15.2	1533	No	No
15 Aug	0853-1020	732	0817	Yes	Yes
	1022-1140	732	1105	Yes	Yes
	1151-1220	30.5	1156	No	No
	1406-1535	305	1354	Yes	Yes
	1537-1656	305	1524	Yes	Yes
	1700-1744	152	1524	Yes	Yes
	1746-1823	152	1524	Yes	Yes

Table 2. Results of applying method to all of the San Diego 3 GHz data

* Aircraft did not go beyond radar horizon

SAN NICOLAS TO SAN CLEMENTE

A dual frequency propagation link was established between the islands of San Clemente and San Nicolas. The transmitter was located on the eastern end of San Nicolas at 3 m MSL, 86.7 km from the receiving antenna situated at 218 m MSL on San Clemente. The frequencies used were in both S-band (2.7 GHz) and X-band (9.6 GHz).

Figure 3 shows several typical refractivity (N) and modified refractivity (M) profiles and associated duct regions if present for the San Nicolas to San Clemente data. Both surface-based and elevated ducts are present. Figures 4 and 5 show the measured path loss and fading as a function of time for the S and X band frequencies respectively. The diffraction level indicated by the lower dashed line is the path loss expected at San Clemente under standard atmospheric conditions.

Refractivity profiles were determined from radiosonde data collected at both islands during the operation. The near-standard profile seen in figure 3d is the result of a well mixed atmosphere brought about by the passage of a cold front through the area. The cool air mass had no low ducts and the signal levels decreased to the normal diffraction levels as seen in figures 4 and 5.

Tables 3 and 4 show the results of applying the subject method of this study to the S and X band respectively of all the San Nicolas to San Clemente data. All of the San Nicolas to San Clemente data is found in reference 7.

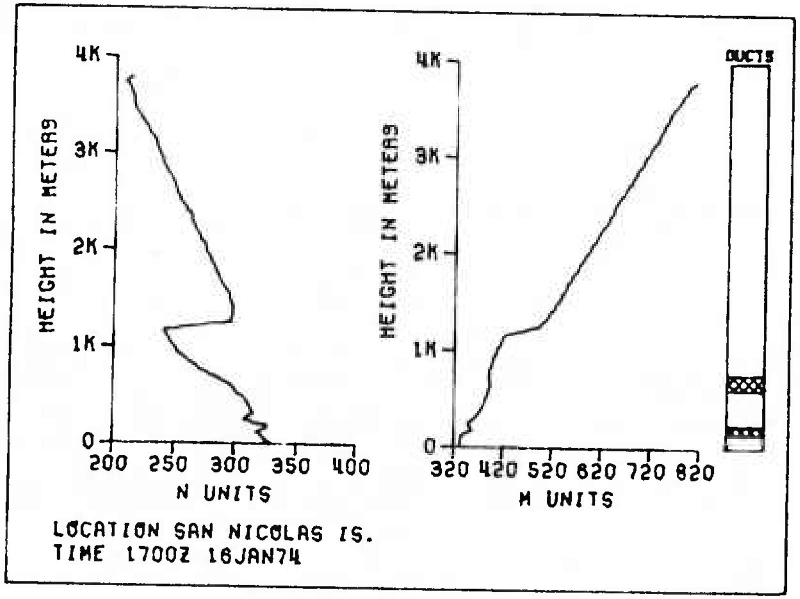
HEIGHT IN METERS
4K
3K
2K
1K
0
200 250 300 350 400
N UNITS
HEIGHT IN METERS
4K
3K
2K
1K
0
320 420 520 620 720 820
M UNITS
DUCTS
LOCATION SAN NICOLAS IS.
TIME 1700Z 16JAN74

a

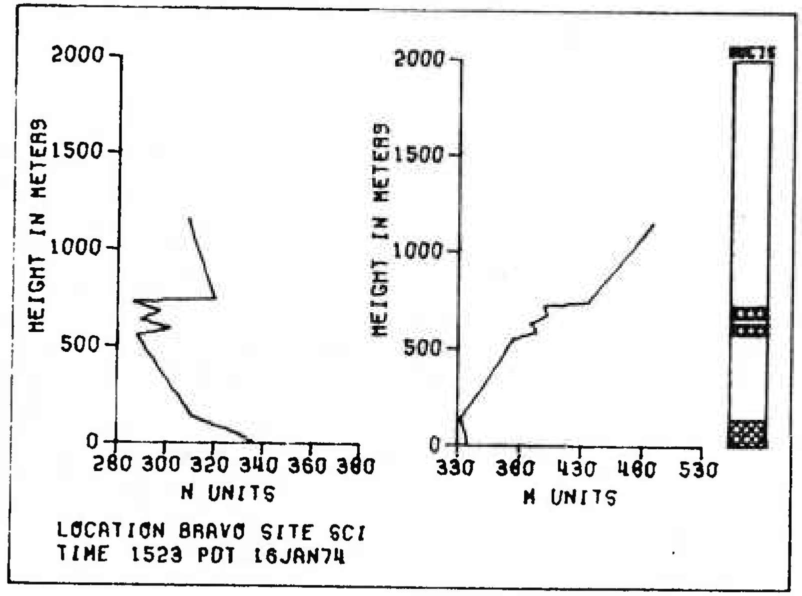
HEIGHT IN METERS
2000
1500
1000
500
0
280 300 320 340 360 380
N UNITS
HEIGHT IN METERS
2000
1500
1000
500
0
330 360 430 460 530
M UNITS
DUCTS
LOCATION BRAVO SITE SCI
TIME 1523 PDT 16JAN74

c

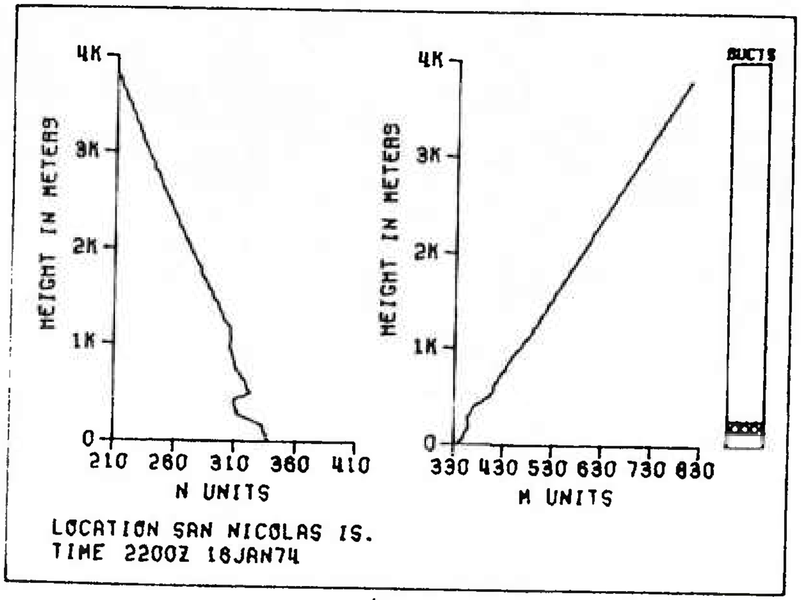
HEIGHT IN METERS
4K
3K
2K
1K
0
210 260 310 360 410
N UNITS
HEIGHT IN METERS
4K
3K
2K
1K
0
330 430 530 630 730 830
M UNITS
DUCTS
LOCATION SAN NICOLAS IS.
TIME 2200Z 16JAN74

b

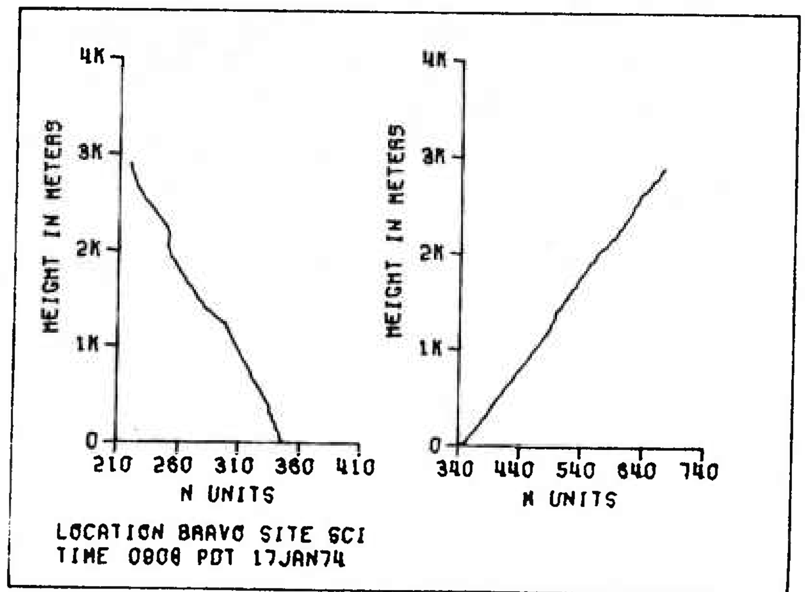
HEIGHT IN METERS
4K
3K
2K
1K
0
210 260 310 360 410
N UNITS
HEIGHT IN METERS
4K
3K
2K
1K
0
340 440 540 640 740
M UNITS
LOCATION BRAVO SITE SCI
TIME 0808 PDT 17JAN74

d

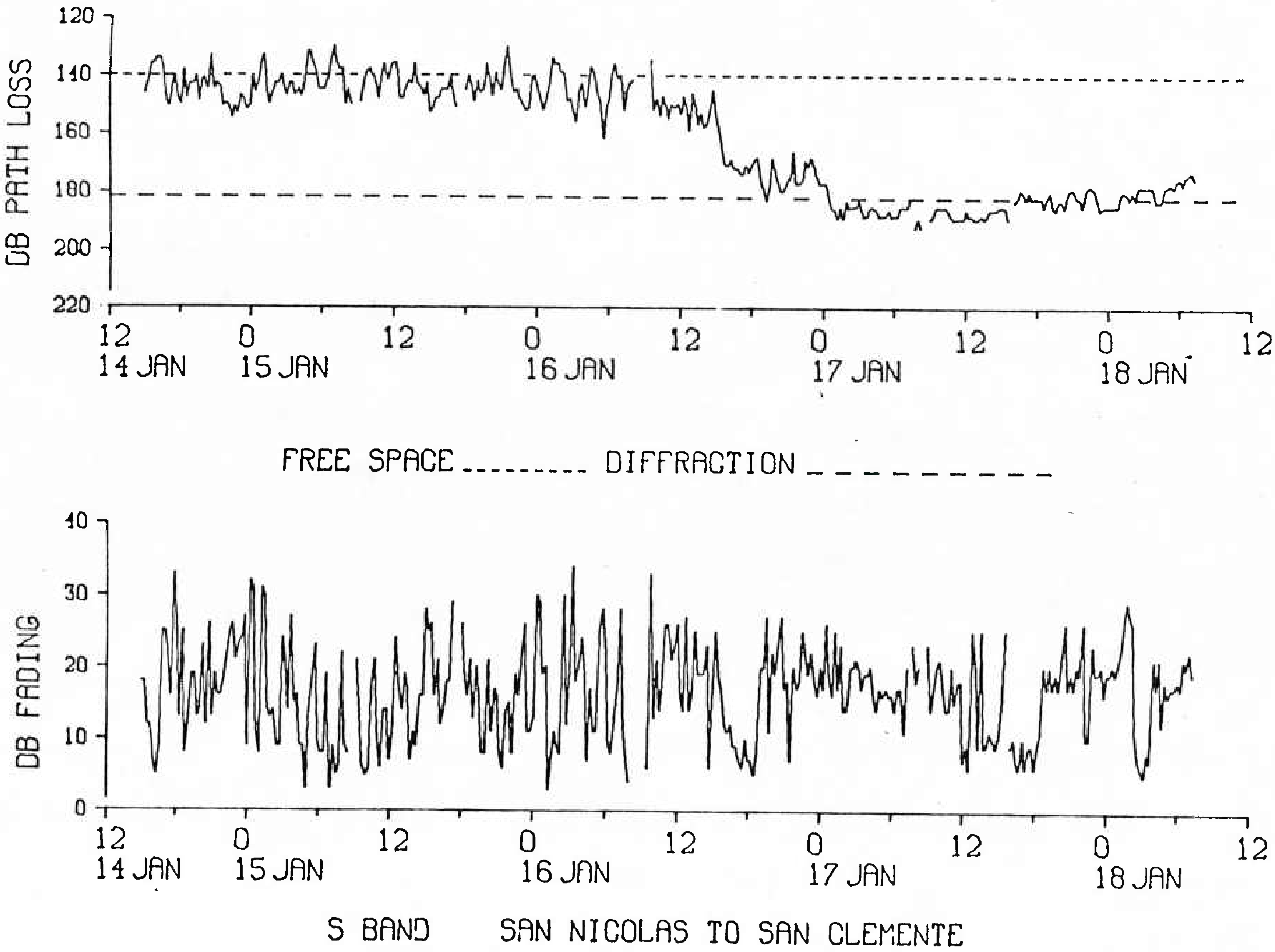

Figure 4. S band Jan Period path loss and fading versus time. (Ref. 7)

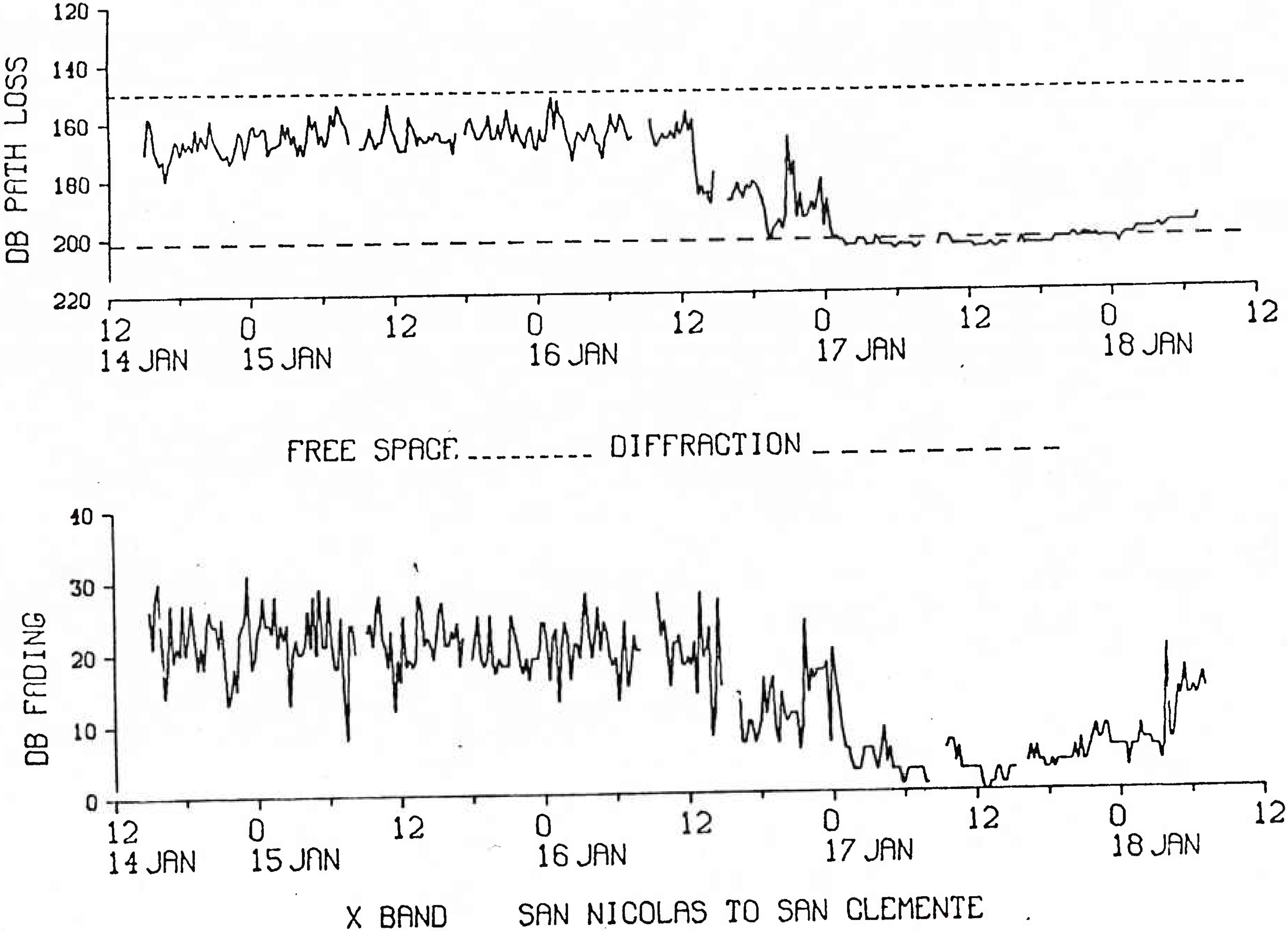

Figure 5 X band Jan Period path loss and fading versus time. (Ref. 7)

Refractivity Obs.			Enhancement		Refractivity Obs.			Enhancement	
Date	Time	Place	Pred	Obs	Date	Time	Place	Pred	Obs
6 Nov 73	0910	SN	No	No	16 Jan 74	0913	SC	Yes	Yes
	1230	SN	No	No		1000	SN	Yes	Yes
	1445	SN	No	No		1500	SN	Yes	No
7 Nov	0845	SN	No	No		1523	SC	Yes	No
	1513	SN	Yes	Yes	17 Jan	0908	SC	No	No
8 Nov	0850	SN	No	No		0940	SN	No	No
	1005	SC	No	No		1500	SN	No	No
	1230	SN	No	No		1514	SC	No	No
	1500	SN	Yes	No	18 Jan	1000	SN	No	No
9 Nov	0755	SN	No	No		1305	SN	No	No
	0930	SC	No	No	11 Feb	0945	SN	Yes	Yes
	1000	SN	No	No		1515	SN	Yes	Yes
	1400	SN	Yes	No	12 Feb	0919	SC	No	No
	1417	SC	No	No		1000	SN	No	No
10 Nov	0925	SC	Yes	Yes		1505	SN	No	No
11 Nov	0930	SC	Yes	Yes		1705	SC	No	No
	2146	SC	Yes	Yes	13 Feb	0731	SC	No	No
12 Nov	0810	SC	No	No		1000	SN	No	No
	1025	SN	Yes	No		1500	SN	No	No
	1330	SN	No	No		1703	SC	No	No
	2050	SC	Yes	No	14 Feb	0721	SC	Yes	No
14 Jan 74	0940	SN	Yes	Yes		1037	SN	No	No
	1500	SN	No	Yes		1500	SN	No	No
15 Jan	1000	SN	Yes	Yes		1703	SC	No	No
	1130	SN	Yes	Yes	15 Feb	1015	SN	Yes	Yes
	1432	SC	Yes	Yes		1400	SN	Yes	Yes
	1500	SN	Yes	Yes					

Table 3. Results of applying method to San Nicolas to San Clemente S-band data. Data is path loss as a function of time. All times are Pacific Standard Time. SN= San Nicolas SC= San Clemente

Refractivity Obs.			Enhancement		Refractivity Obs.			Enhancement	
Date	Time	Place	Pred	Obs	Date	Time	Place	Pred	Obs
6 Nov73	0910	SN	No	No	16 Jan 74	0913	SC	Yes	Yes
	1230	SN	No	No		1000	SN	Yes	Yes
	1445	SN	No	No		1500	SN	Yes	No
7 Nov	0845	SN	No	No		1523	SC	Yes	No
	1513	SN	Yes	Yes	17 Jan	0908	SC	No	No
8 Nov	0850	SN	No	No		0940	SN	No	No
	1005	SC	No	No		1500	SN	No	No
	1230	SN	No	No		1514	SC	No	No
	1500	SN	Yes	No	18 Jan	1000	SN	No	No
9 Nov	0755	SN	No	No		1305	SN	No	No
	0930	SC	No	No	11 Feb	0945	SN	Yes	Yes
	1000	SN	No	No		1515	SN	Yes	Yes
	1400	SN	Yes	No	12 Feb	0919	SC	No	Yes
	1417	SC	No	No		1000	SN	No	Yes
10 Nov	0925	SC	Yes	Yes		1505	SN	No	Yes
11 Nov	0930	SC	Yes	Yes		1705	SC	No	Yes
	2146	SC	Yes	Yes	13 Feb	0731	SC	No	Yes
12 Nov	0810	SC	No	No		1000	SN	No	Yes
	1025	SN	Yes	Yes		1500	SN	No	Yes
	1330	SN	No	Yes		1703	SC	No	Yes
	2050	SC	Yes	No	14 Feb	0721	SC	Yes	No
14 Jan 74	0940	SN	Yes	Yes		1037	SN	No	No
	1500	SN	No	Yes		1500	SN	No	No
15 Jan	1000	SN	Yes	Yes		1703	SC	No	No
	1130	SN	Yes	Yes	15 Feb	1015	SN	Yes	Yes
	1432	SC	Yes	Yes		1400	SN	Yes	Yes
	1500	SN	Yes	Yes					

Table 4. Results of applying method to San Nicolas to San Clemente X-Band. Data is path loss as a function of time. All times Pacific Standard time. SN = San Nicolas SC = San Clemente

SAN DIEGO HIGH ALTITUDE DATA

This data consists of field strength distributions at frequencies of 418 and 1089 MHz using a transmitter equipped Navy jet aircraft making constant altitude flights entirely over the ocean at elevations ranging from 8.7 to 11.9 km during the period from January 1953 to January 1955.

The receivers were located on a cliff overlooking the ocean with an antenna height of 33 m MSL. Measurements were made as the aircraft flew from a point 548.5 km from the receivers on a straight course toward the receivers.

Figure 6 shows a typical M profile which in this case was calculated from the B profile seen in figure 7 using the relationship $M = .118\ h + B$ where h is altitude in meters. B units are actual index-of-refraction units, n, modified such that a standard atmosphere is represented by a vertical line.

Figure 7 shows a typical example of the measurements of field strength in DB relative to free space as a function of distance for both frequencies used in this experiment. It also corresponds in time to the M profile of figure 6.

Tables 5 and 6 show the results of the prediction method for the 418 and 1089 MHz signals respectively. All of the San Diego high altitude data is found in reference 8.

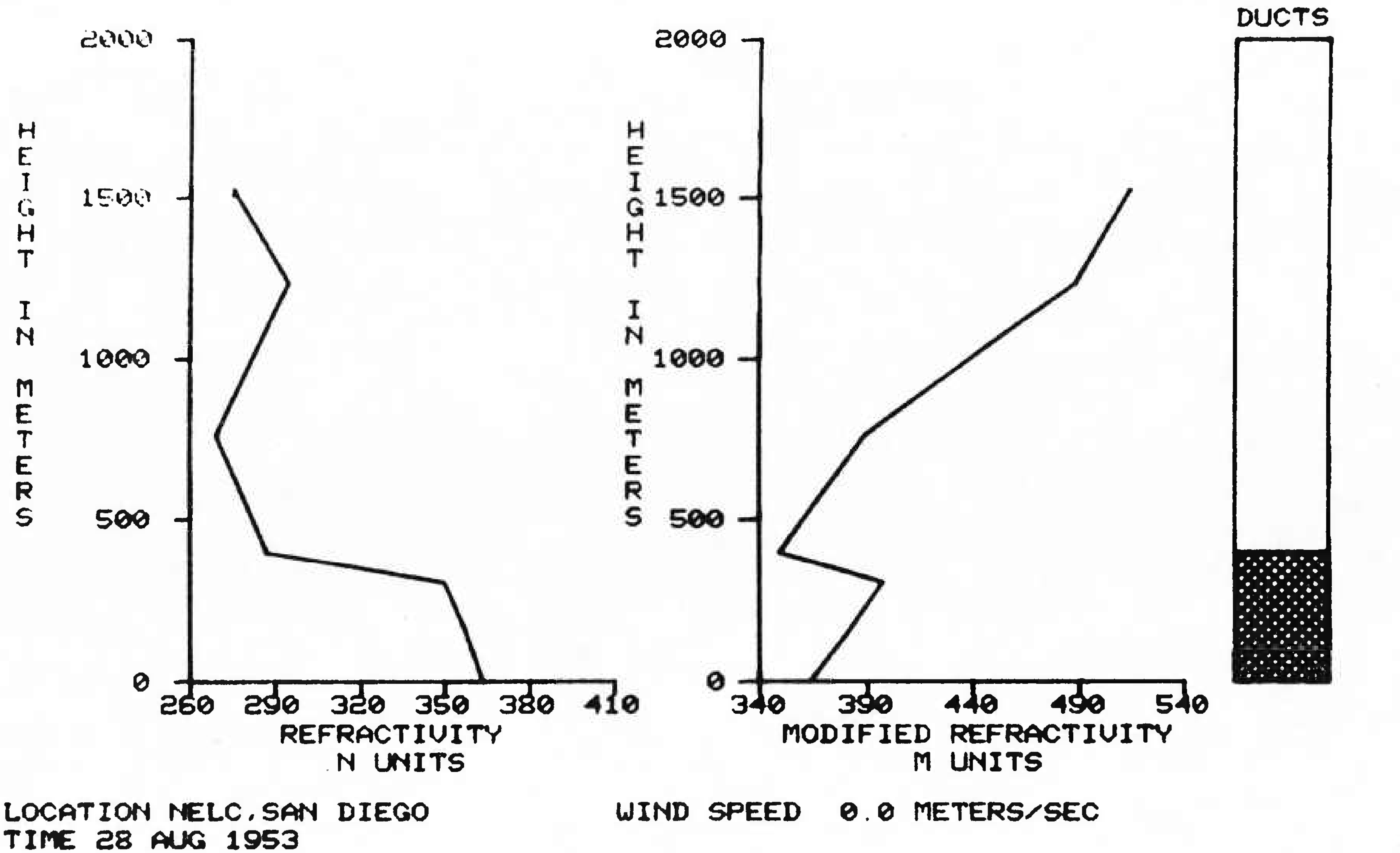

Figure 6. Sample refractivity and modified refractivity profiles calculated from San Diego high altitude data (Ref. 8)

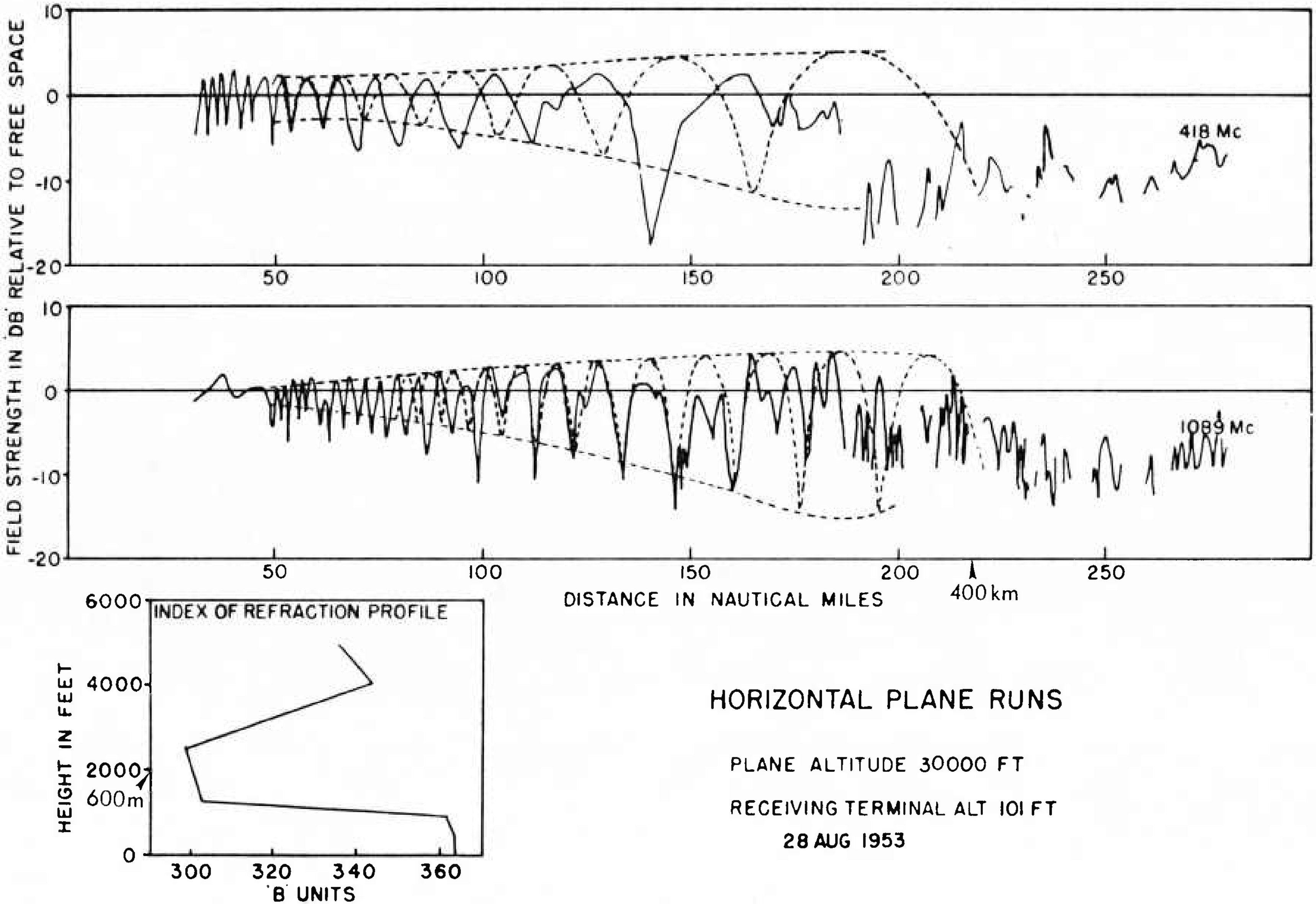

Figure 7. Sample plots of field strength as a function of range from San Diego high altitude data. (Ref. 8)

Flight Data		Enhancement	
Date	Altitude (m)	Pred.	Obs.
10 Mar 53	8689	No	No
8 Jul	10061	Yes	Yes
28 Aug	9146	Yes	Yes
22 Sep	11890	No	Yes
8 Dec	9146	No	--*
15 Dec	9146	Yes	Yes
7 Jan 54	9146	No	No
28 Sep 54	9908	No	Yes

Table 5. Results of applying method to San Diego high altitude data. 418 MHz

* Observation not available

Flight Data		Enhancement	
Date	Altitude (m)	Pred.	Obs.
10 Mar 53	8689	No	No
8 Jul	10061	Yes	Yes
28 Aug	9146	Yes	Yes
22 Sep	11890	No	No
8 Dec	9146	No	Yes
15 Dec	9146	Yes	Yes
7 Jan 54	9146	No	No
28 Sep 54	9908	No	Yes

Table 6. Results of applying method to San Diego high altitude data. 1089 MHz

GUADALUPE DATA

Over-water transmission studies were made utilizing a PBY-5A aircraft, equipped with transmitters, which flew between San Diego and Guadalupe Island approximately 512 km to the south of San Diego. Transmissions were made on 65, 170, 520 and 3300 MHz. Amplitudes of the received signals were recorded simultaneously at elevations of 30 and 152 m. Variations of the strength of the radio fields between San Diego and Guadalupe Island were recorded during data periods from June 1947 and June 1949.

Figure 8 shows an M profile which was calculated from the typical B profiles used in this experiment using the previously mentioned relationship. Figure 9 shows an example of signal strength measurements in DB relative to free space as a function of altitude for the four frequencies used. The shaded area in the meteorological profiles denotes the trapping layer as determined by the B profile. Table 7 shows the results of applying the horizontal homogeneity test using the 3300 MHz data at both receiver heights. The Guadalupe data is not published, however a sample is found in reference 9.

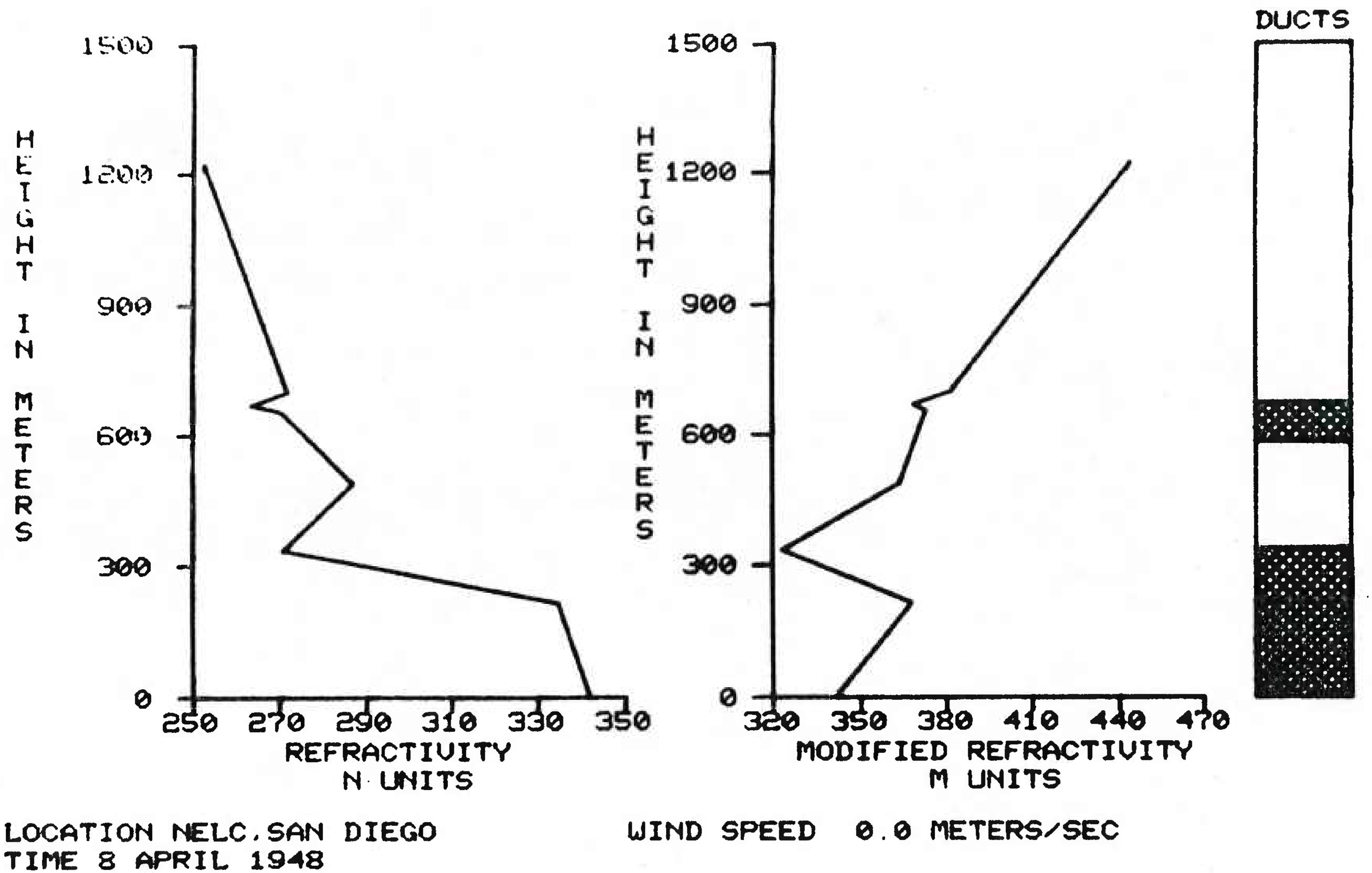

Figure 8. Sample refractivity and modified refractivity from Guadalupe data (Ref. 9)

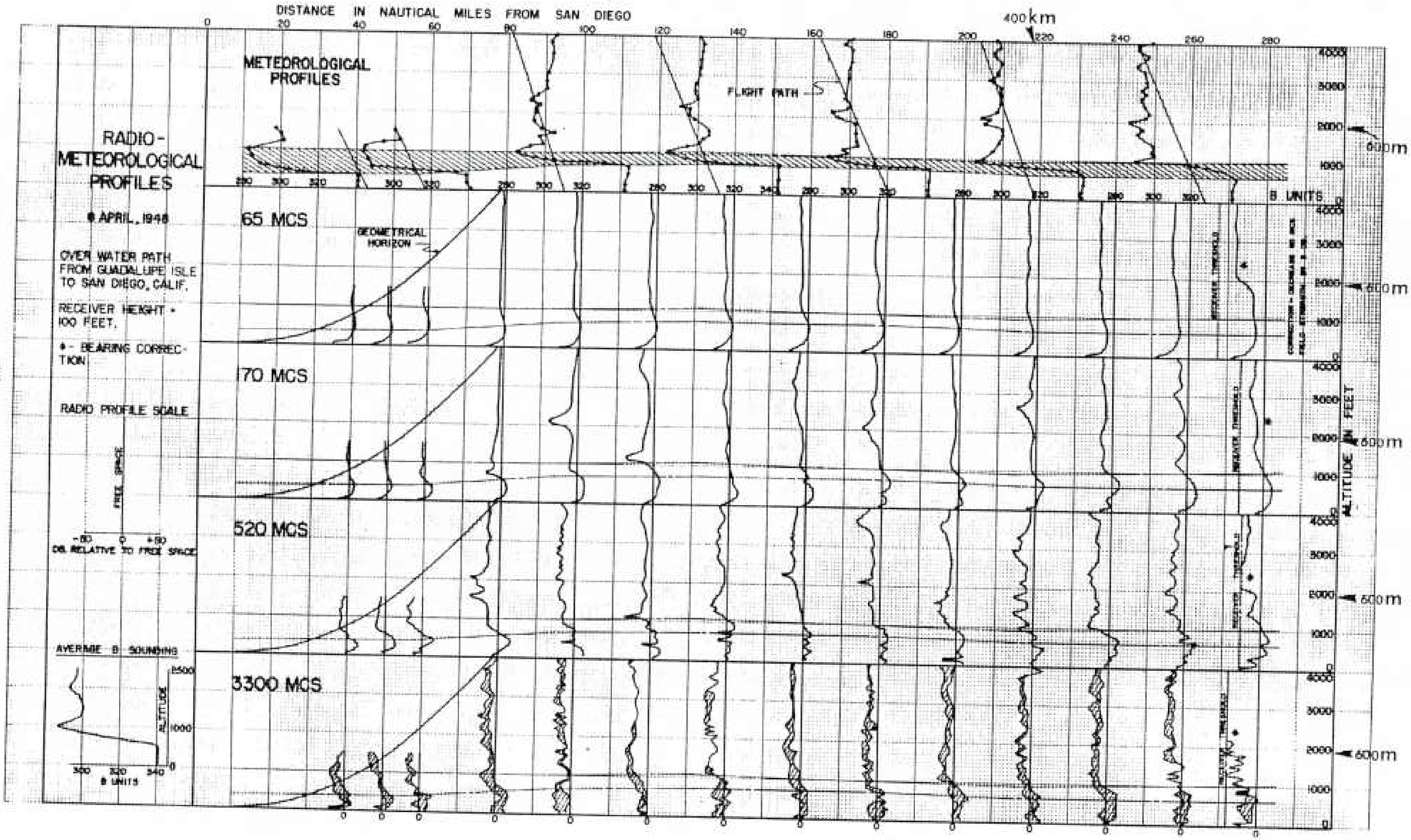

Figure 9. Sample radio profiles from Guadalupe data (Ref. 9)

Date	Receiver Ht.(m)	Refractivity Obs. Distance (km)	Enhancement Pred	Enhancement Obs
13 May 47	30.5	82	No	No
3 Jun	30.5	109.8	No	No
3 Jun	152.5	109.8	No	No
25 Sep	30.5	139	Yes	Yes
5 Nov	30.5	165	No	No
5 Nov	152.5	165	No	No
13 Nov	30.5	141	No	No
13 Nov	152.5	141	Yes	Yes
12 Mar 48	30.5	90	Yes	Yes
12 Mar	152.5	90	Yes	Yes
17 Mar	30.5	75	No	No
17 Mar	152.5	75	No	No
8 Apr	30.5	127	Yes	Yes
8 Apr	152.5	127	Yes	Yes
22 Jun 49	30.5	55	Yes	Yes
22 Jun	152.5	55	Yes	Yes

Table 7. Results of applying method to Guadalupe data. Distance in km is to point along flight path where sounding was taken.

CANTERBURY DATA

The Canterbury data was obtained by radio-meteorological measurements taken between September 1946 and November 1947 on the South Island of New Zealand. The experiment was prompted by the anomalous radio propagation observed during World War II. Radar receivers on 3300 and 10,000 MHz were situated at the coast at elevations of approximately 8 and 26 meters each. Anson aircraft carried transmitters on both channels and flew at various altitudes between 6 and 915 m on a path perpendicular to the coastline out to as far as 180 km. Meteorological data was obtained over land and water to determine modified refractivity (M) profiles at points from 20 km inland every 20 km along the flight path to 160 km out to sea. Aircraft and a surface vessel were used for overwater measurements.

Figure 10 shows a set of profiles for a typical day of measurements. In most cases the 20 km over-water profile was used to make predictions. Figure 11 shows an example of typical radar measurements made at Canterbury plotted as signal strength in dB as a function of range. F.S.L. denotes the free space level. Tables 8 and 9 show the results of this study in both S and X band respectively as applied to the Canterbury data. All of the Canterbury data is found in reference 10.

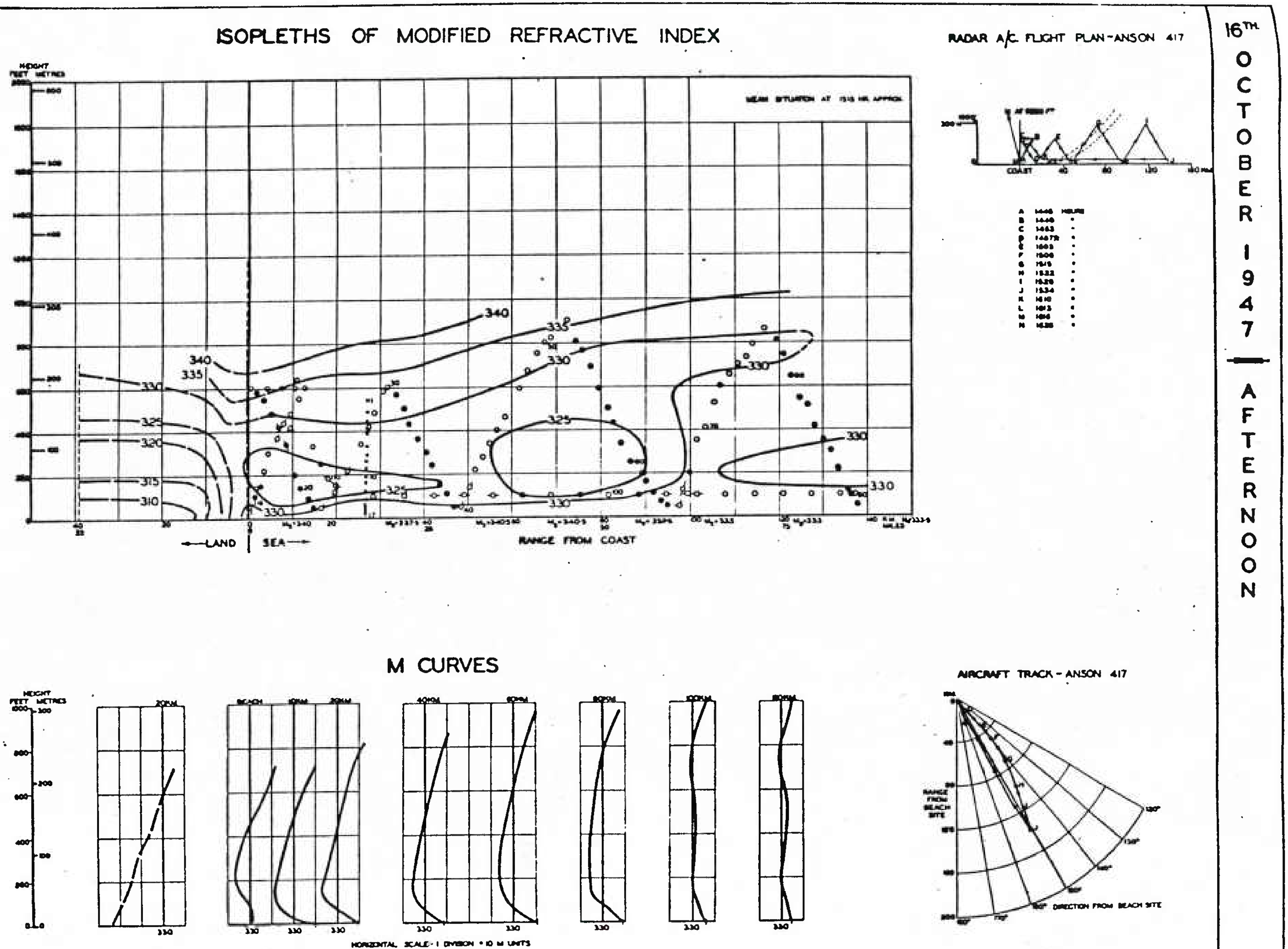

Figure 10. Sample refractivity measurements from Canterbury data (Ref. 10)

HEIGHT GAIN CURVES

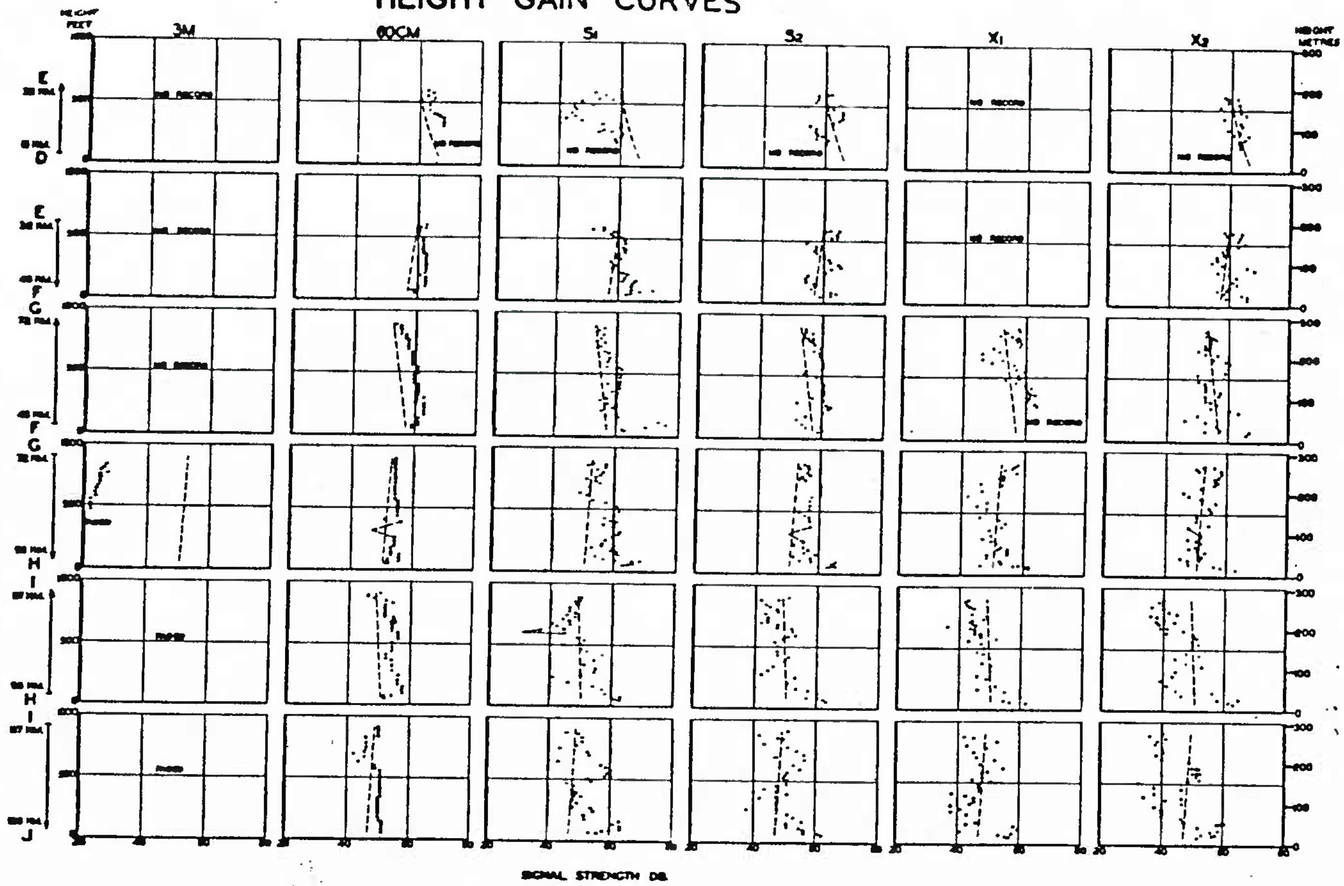

100 FT. RUN IN LEG J-K 138 KM – 215 KM.

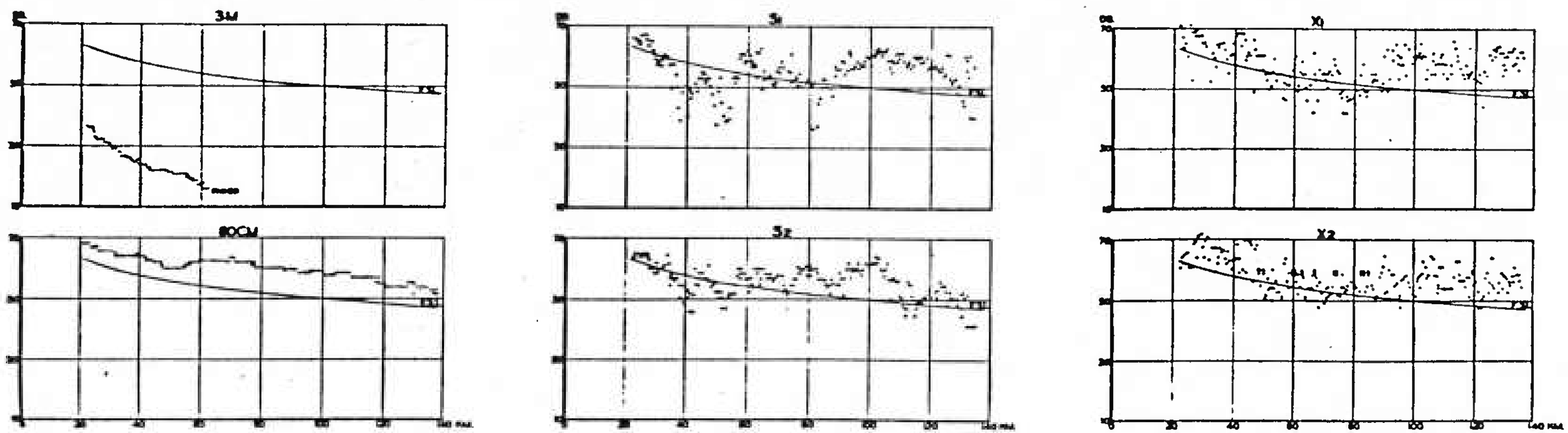

16TH OCTOBER 1947 — AFTERNOON

	Flight Data			Refract Obs	Enhancement	
Date	Time	Alt.(m)	Acft	Dist (km)	Pred	Obs
14 Oct 46	A	30.5	422	20	Yes	---
15 Oct	A	183	419	20	Yes	Yes
24 Oct	A	61	422	Beach	Yes	Yes
24 Oct	P	61	419	16	Yes	---*
4 Nov	P	61	415	20	Yes	Yes
5 Nov	A	61		6.5	Yes	No
26 Nov	P	61	419	20	Yes	---
8 Dec	P	15.2	415	Beach	Yes	Yes
8 Dec	P	30.5	415	Beach	Yes	Yes
15 Dec	P	61	419	20	Yes	Yes
22 Jan 47	P	--	419	20	Yes	---*
27 Jan	P	15.2	419	20	Yes	Yes
6 Feb	P	15.2	419	20	No	No
19 Feb	P	152	422	Beach	No	No
19 Feb	P	15.2	419	20	Yes	No
20 Feb	P	15.2	422	20	Yes	Yes
23 Feb	P	15.2	422	20	Yes	Yes
24 Feb	P	15.2	422	20	Yes	Yes
4 Mar	P	15.2	415	20	Yes	Yes
2 Apr	P	15.2	422	20	Yes	Yes
2 Apr	P	152	422	20	Yes	Yes
8 Apr	P	152	422	20	Yes	Yes
4 May	P	15.2	422	20	Yes	No
6 May	P	15.2	422	20	Yes	Yes
7 May	P	15.2	422	20	Yes	Yes
7 May	P	30.5	415	20	Yes	Yes
8 May	P	15.2	422	20	Yes	No
13 May	P	15.2	422	20	Yes	Yes
19 May	A	15.2	422	20	Yes	Yes
19 May	P	15.2	422	20	Yes	No
28 May	P	15.2	422	20	Yes	Yes
16 Jun	P	152	417	20	Yes	No
18 Jun	P	305	417	20	Yes	Yes
19 Jun	P	15.2	417	20	Yes	Yes
23 Jun	P	30.5	417	20	Yes	Yes
24 Jun	P	15.2	417	20	Yes	Yes
25 Jun	P	76.2	419	20	No	No
10 Jul	P	15.2	419	20	Yes	Yes
11 Jul	A	15.2	417	20	Yes	---
15 Jul	P	15.2	417	20	Yes	Yes
1 Aug	P	15.2	417	20	Yes	Yes
2 Aug	P	15.2	417	20	Yes	Yes
3 Aug	P	15.2	417	20	Yes	Yes
5 Aug	P	15.2	417	20	Yes	Yes

Table 8. Results of applying method to Canterbury S band data. Time is AM or PM denoted by A or P respectively. Distance is measured along path seaward from beach. * Acft did not go beyond radar horizon.

Flight Data				Refract Obs	Enhancement	
Date	Time	Alt.(m)	Acft	Dist (km)	Pred	Obs
6 Aug 47	P	15.2	422	20	Yes	Yes
14 Aug	P	15.2	417	20	Yes	No
1 Sep	P	15.2	422	60	Yes	Yes
4 Sep	P	15.2	417	20	Yes	Yes
7 Sep	P	15.2	419	Beach	Yes	Yes
9 Sep	P	15.2	419	20	Yes	Yes
15 Sep	P	15.2	417	20	Yes	Yes
15 Sep	P	15.2	417	20	Yes	Yes
17 Sep	P	15.2	417	20	Yes	Yes
24 Sep	A	15.2	417	20	Yes	Yes
24 Sep	P	15.2	417	20	Yes	Yes
24 Sep	P	21.3	419	20	Yes	Yes
29 Sep	P	15.2	422	20	Yes	No
29 Sep	P	152	417	20	Yes	Yes
6 Oct	A	76.2	417	20	Yes	Yes
6 Oct	P	15.2	417	20	Yes	Yes
16 Oct	A	15.2	417	20	Yes	Yes
16 Oct	P	30.5	417	20	Yes	Yes
17 Oct	A	30.5	417	20	Yes	No
19 Oct	P	15.2	417	20	Yes	Yes
20 Oct	A	15.2	419	20	Yes	Yes
20 Oct	P	15.2	419	20	Yes	Yes
21 Oct	A	45.7	417	20	Yes	Yes
23 Oct	A	15.2	417	20	Yes	Yes
23 Oct	P	30.5	417	20	Yes	Yes
24 Oct	A	152	419	20	Yes	No
3 Nov	A	15.2	419	20	Yes	Yes
3 Nov	P	15.2	419	20	Yes	Yes
4 Nov	A	15.2	417	20	Yes	Yes
4 Nov	P	15.2	417	20	Yes	Yes
5 Nov	A	15.2	417	20	Yes	Yes
25 Nov	A	15.2	419	15	Yes	Yes
25 Nov	P	15.2	419	20	Yes	Yes
26 Nov	A	15.2	417	20	Yes	Yes
26 Nov	P	30.5	417	20	Yes	Yes
27 Nov	A	15.2	417	20	Yes	Yes

Table 8. Continued

Date	Flight Data Time	Alt.(m)	Acft	Refract Obs Dist (km)	Enhancement Pred	Enhancement Obs
14 Oct 46	A	30.5	422	20	Yes	Yes
15 Oct	A	183	419	20	Yes	Yes
24 Oct	A	61	422	Beach	Yes	Yes
24 Oct	P	61	419	16	Yes	---*
4 Nov	P	61	415	20	Yes	Yes
5 Nov	A	61		6.5	Yes	No
26 Nov	P	61	419	20	Yes	---
8 Dec	P	15.2	415	Beach	Yes	---
8 Dec	P	30.5	415	Beach	Yes	---
15 Dec	P	61	419	20	Yes	---
22 Jan 47	P		419	20	Yes	---*
27 Jan	P	15.2	419	20	Yes	---
6 Feb	P	15.2	419	20	No	No
19 Feb	P	152	422	Beach	No	No
19 Feb	P	15.2	419	20	Yes	No
20 Feb	P	15.2	422	20	Yes	Yes
23 Feb	P	15.2	422	20	Yes	Yes
24 Feb	P	15.2	422	20	Yes	Yes
4 Mar	P	15.2	415	20	Yes	Yes
2 Apr	P	15.2	422	20	Yes	Yes
2 Apr	P	15.2	422	20	Yes	Yes
8 Apr	P	152	422	20	Yes	Yes
4 May	P	15.2	422	20	Yes	No
6 May	P	15.2	422	20	Yes	Yes
7 May	P	15.2	422	20	Yes	Yes
7 May	P	30.5	415	20	Yes	Yes
8 May	P	15.2	422	20	Yes	Yes
13 May	P	15.2	422	20	Yes	Yes
19 May	A	15.2	422	20	Yes	Yes
19 May	P	15.2	422	20	Yes	No
28 May	P	15.2	422	20	Yes	Yes
16 Jun	P	152	417	20	Yes	Yes
18 Jun	P	305	417	20	Yes	Yes
19 Jun	P	15.2	417	20	Yes	Yes
23 Jun	P	30.5	417	20	Yes	Yes
24 Jun	P	15.2	417	20	Yes	Yes
25 Jun	P	76.2	419	20	No	No
10 Jul	P	15.2	419	20	Yes	Yes
11 Jul	A	15.2	417	20	Yes	Yes
15 Jul	P	15.2	417	20	Yes	Yes
1 Aug	P	15.2	417	20	Yes	Yes
2 Aug	P	15.2	417	20	Yes	Yes
3 Aug	P	15.2	417	20	Yes	Yes
5 Aug	P	15.2	417	20	Yes	Yes

Table 9. Results of applying method to Canterbury X band data. Time is AM or PM denoted by A or P respectively. Distance is measured along path seaward from beach. * Acft did not go beyond radar horizon.

	Flight Data			Refract Obs	Enhancement	
Date	Time	Alt.(m)	Acft	Dist (km)	Pred	Obs
6 Aug 47	P	15.2	422	20	Yes	Yes
14 Aug	P	15.2	417	20	Yes	No
1 Sep	P	15.2	422	60	Yes	Yes
4 Sep	P	15.2	417	20	Yes	Yes
7 Sep	P	15.2	419	Beach	Yes	Yes
9 Sep	P	15.2	419	20	Yes	Yes
15 Sep	P	15.2	417	20	Yes	Yes
15 Sep	P	15.2	417	20	Yes	Yes
17 Sep	P	15.2	417	20	Yes	Yes
24 Sep	A	15.2	417	20	Yes	Yes
24 Sep	P	15.2	417	20	Yes	---
24 Sep	P	21.3	419	20	Yes	Yes
29 Sep	P	15.2	422	20	Yes	Yes
29 Sep	P	152	417	20	Yes	Yes
6 Oct	A	76.2	417	20	Yes	Yes
6 Oct	P	15.2	417	20	Yes	Yes
16 Oct	A	15.2	417	20	Yes	Yes
16 Oct	P	30.5	417	20	Yes	Yes
17 Oct	A	30.5	417	20	Yes	No
19 Oct	P	15.2	417	20	Yes	---
20 Oct	A	15.2	419	20	Yes	Yes
20 Oct	P	15.2	419	20	Yes	Yes
21 Oct	A	45.7	417	20	Yes	Yes
23 Oct	A	15.2	417	20	Yes	Yes
23 Oct	P	30.5	417	20	Yes	Yes
24 Oct	A	152	419	20	Yes	Yes
3 Nov	A	15.2	419	20	Yes	Yes
3 Nov	P	15.2	419	20	Yes	Yes
4 Nov	A	15.2	417	20	Yes	Yes
4 Nov	P	15.2	417	20	Yes	Yes
5 Nov	A	15.2	417	20	Yes	Yes
25 Nov	A	15.2	419	15	Yes	Yes
25 Nov	P	15.2	419	20	Yes	Yes
26 Nov	A	15.2	417	20	Yes	Yes
26 Nov	P	30.5	417	20	Yes	Yes
27 Nov	A	15.2	417	20	Yes	Yes

Table 9. Continued

CONCLUSIONS

A prediction model which assumes horizontal homogeneity of the radio refractive index was evaluated. The results achieved by applying this model and comparing the predictions with observed data showed that in the vast majority of cases predictions based on the assumption of horizontal homogeneity of the refractive index are accurate. Due to the validity of these predictions it is concluded that predictions of radio field strength enhancement beyond the horizon, based on a single refractivity profile, and the assumption of horizontal homogeneity can be expected to be correct a majority of the time.

ACKNOWLEDGEMENT

The author wishes to express his appreciation for the expert advice of H. V. Hitney throughout the preparation of this report and for the constructive ideas of V. R. Noonkester.

REFERENCES

1. Hitney, H. V., Propagation Modelling in the Evaporation Duct, NELC TR 1947, 1 April 1975

2. Richter, J. H. and H. V. Hitney, The Effect of the Evaporation Duct on Microwave Propagation, NELC TR 1949, 17 April 1975

3. Richter, J. H. and H. V. Hitney, Antenna Heights for Optimum Utilization of the Oceanic Surface Evaporation Duct, Part I, NELC TN 2031, 4 May 1972

4. Richter, J. H. and H. V. Hitney, Antenna Heights for Optimum Utilization of the Oceanic Surface Evaporation Duct, Part II, NELC TN 2371 10 May 1973

5. Richter, J. H. and H. V. Hitney, Antenna Heights for Optimum Utilization of the Oceanic Surface Evaporation Duct, Part III, NELC TN 2569, 26 November 1973

6. Anderson, K. D. and D. R. Jensen and M. L. Phares, Propagation Measurements at 3 GHz in the San Diego Offshore Area, NELC TN 2874, 20 January 1975

7. Anderson, K. D. and H. V. Hitney, D. R. Jensen and J. H. Richter, Propagation Measurements Between San Clemente and San Nicolas Islands, NELC TN 2768, 12 August 1974

8. Hopkins, R. U. F., and J. B. Smyth and L. G. Trolese, The Effect of Superrefraction on the High Altitude Coverage of Ground Based Radar, NEL TR 741, 12 December 1956

9. Trolese, L. G., "Tropospheric Propagation Characteristics", Symposium on Tropospheric Wave Propagation, 17-26, NE 120301 Report 173, 25-29 July 1949

10. Report of Factual Data from the Canterbury Project, Vols I-III, Department of Scientific and Industrial Research, Wellington, New Zealand, 1951

BIBLIOGRAPHY

Bean, B. R. and E. J. Dutton, Radio Meteorology, National Bureau of Standards Monograph 92, March 1, 1966

Bean, B. R. and B. A. Cahoon, "The Effect of Atmospheric Horizontal Homogeneity upon Ray Tracing", Journal of Research of the National Bureau of Standards 63D (Radio Propagation), 287-292, No. 3, November - December 1959

Clarke, L. C., Operational Radar Meteorology Fleet Numerical Weather Facility TN No. 27 March 1967

Kerr, D. E., Propagation of Short Radio Waves, McGraw-Hill Book Company, Inc., New York, Toronto, London, 1951

Noonkester, V. R. and H. V. Hitney, Synoptic Prediction of Meteorological Factors Affecting Tropospheric Radio Propagation, NELC TR 1934, 1 October 1974

Reed, H. R. and C. M. Russell, Ultra High Frequency Propagation, Second Edition, Boston Technical Publishers, Inc., Cambridge, Massachusetts, 1966

Sherar, R. C. and J. Rosenthal, "Don't Fall in the Radar Hole", U. S. Naval Institute Proceedings, 55-66, December, 1973